

FS electromagnetic characterisation of a flexible and scalable X-band RAM

ISSN 1751-8725
 Received on 30th May 2017
 Revised 15th December 2017
 Accepted on 17th January 2018
 E-First on 12th March 2018
 doi: 10.1049/iet-map.2017.0482
 www.ietdl.org

Anibal Aguirre¹ ✉, Cristian Torres de Pedro², Borja Plaza Gallardo³, David Poyatos Martínez², David Escot Bocanegra²

¹Antennas and Propagation Division, Research and Development Institute for Defense (CITEDEF), San Juan Bautista de La Salle 4397 (B1603ALO), Villa Martelli, Buenos Aires, Argentina

²National Institute for Aerospace Technology (INTA), Ctra Ajalvir km 4, Torrejón de Ardoz, 28850 Madrid, Spain

³Electronic Warfare Area, ISDEFE, c/Beatriz de Bobadilla, 3, 28040 Madrid, Spain

✉ E-mail: aaguirre@citedef.gob.ar

Abstract: Along the years, RADAR absorbing materials (RAM's) have been widely introduced in aeronautic applications and platforms. However, this kind of materials presents three main problems for certain applications when they are intended to be used in real operations. First, they must be scalable from a laboratory sample to actual size, at a reasonable cost. Second, they must be able to work without metal backing for applications in non-metallic vehicles or other objects which surface might not be flat. Indeed, they should also be flexible and surface adaptable. Finally, their absorbing properties against electromagnetic fields should be preferably characterised under real conditions, that is, in free space (FS), in order to design and fabricate an appropriate material for the intended application. In this study, a self-developed, low-cost, bilayer, X-band RAM, composed of a lower layer of polyaniline silicon rubber and a top layer of silicon rubber with graphite was characterised in a bistatic anechoic chamber called BIANCHA, and the results are presented, analysed and compared with software simulation and with the typical single polarisation waveguide measurement method, showing the adequacy of FS measurements for the development of this type of RAM.

1 Introduction

Research in absorbing materials came together with the early developments of RADAR and a patent of a RADAR absorbing material (RAM) can already be tracked back to 1936 [1]. Now, there is a very wide variety of RAM's [2, 3] with different basic materials [4, 5], bandwidth, absorption level, cost [6, 7] and mechanical properties. Certainly, for aeronautical use, the ideal RAM should be very thin, light, weather resistant and cheap and should obviously behave as a very good microwave absorber [8].

Achieving such a material is not an easy task and practical difficulties occur, particularly for certain applications. The authors are working in the development of RAM's that could be employed as the airship envelope for lighter-than-air vehicles or as a rapid-deployment store to cover a plane on a platform. As a consequence, both flexibility and good performance without using a metal backing are required, and, thus, for instance, carbon fibre fabrics with the necessary conducting properties have been explored [9, 10]. Besides, the amount of material needed for this application implies developments that can enable the laboratory samples to be easily scalable to bigger dimensions at a reasonable cost and maintain the absorbing properties. To meet this objective, it is advantageous to have a composite made up of only one type of filler. Finally, to assess the performance of the developed RAM, the material needs to be tested with a suitable method [11].

In this regard, this paper deals with the characterisation of a flexible absorbing material developed to meet the requirements just presented for the described application, and designed to have a good behaviour at the X-band (8–12 GHz). In the opinion of the authors, the absorbing properties against electromagnetic (EM) fields are better characterised under real conditions, that is, in free space (FS). It is true that one of the most common characterisation approaches is based on the use of waveguides [12], though dielectric probes are also used [13], but when the RAM is a flexible composite material (as in this case), this method does not provide the best characterisation results [14, 15], and then the use of FS methods [16] seems to be preferable. Thus, the main focus of this

work is to show a reliable EM characterisation method of a flexible RAM based on FS measurements in monostatic and bistatic configurations.

This paper is organised as follows. Section 2 gives a short theoretical introduction to RAM behaviour, whereas Section 3 describes the material concept and the elaboration process. Also bistatic anechoic chamber (BIANCHA), the facility where the FS measurements were conducted is presented including a brief description of the different tests performed, namely absorption, permittivity estimation and radar cross-section (RCS) measurements. Section 4 shows and discusses the results including comparisons with waveguide absorption measurements and RCS simulations. Finally, Section 5 draws the final conclusions.

2 Theory

The behaviour of RAM can be derived from the transmission line theory [17]. For the general case, an n-layer RAM backed by a perfect electrical conductor (PEC) (see Fig. 1), the wave impedance of the *i*th layer is given by

$$Z_i = \eta_i \frac{Z_{i-1} + \eta_i \tanh(\gamma_i d_i)}{\eta_i + Z_{i-1} \tanh(\gamma_i d_i)} \quad (1)$$

where η_i , γ_i and d_i in are the characteristic impedance, propagation constant and thickness, respectively, and η_0 is the vacuum impedance ($\approx 377 \Omega$).

The characteristic impedance and the propagation constant are calculated by

$$\eta_i = \sqrt{\frac{\mu_0}{\epsilon_0} \frac{\mu_r}{\epsilon_r}} \quad (2)$$

and

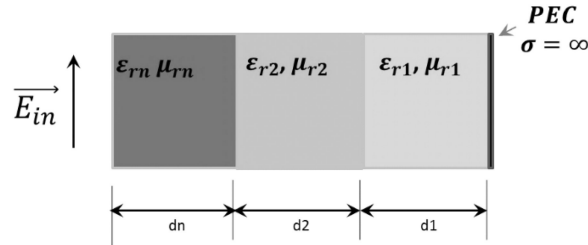


Fig. 1 Generic *i*-layer RAM configuration

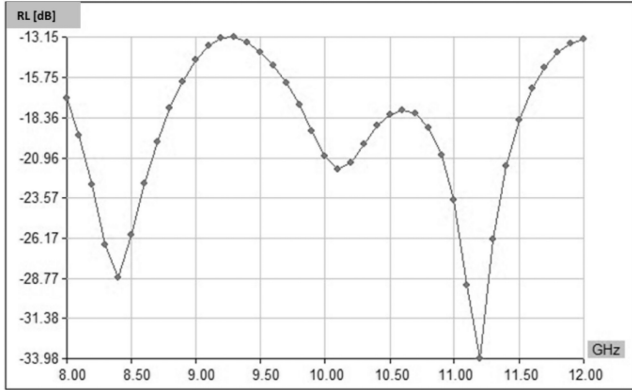


Fig. 2 Computed RL design results

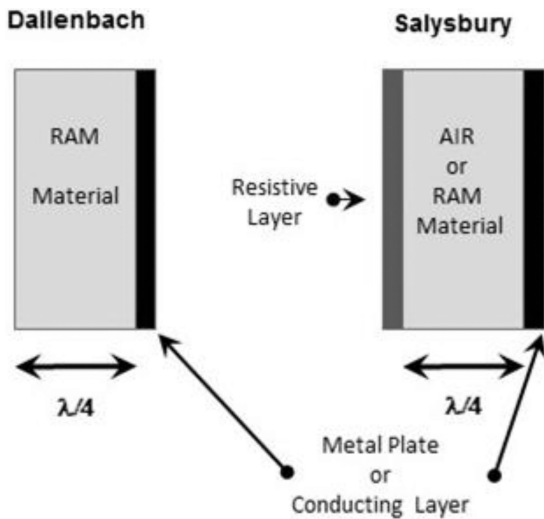


Fig. 3 Typical RAM configurations

$$\gamma_i = \frac{j\omega}{c} \sqrt{\mu_r \epsilon_r} \quad (3)$$

From the transmission line theory, the reflection loss (RL) of the normal incident wave is defined as

$$RL(\text{dB}) = 20 \log_{10} |\Gamma| = \left| \frac{Z_n - \eta_0}{Z_n + \eta_0} \right| \quad (4)$$

For the present paper, the designed RAM has two layers and the RL (dB) can be calculated by [18–20]

$$= 20 \log_{10} \left| \frac{(\sqrt{\mu_1/\epsilon_1} \tanh(\gamma_1 d_1) + (\sqrt{\mu_2/\epsilon_2} \tanh(\gamma_2 d_2))) / \sqrt{((\mu_1 \epsilon_2)/(\epsilon_1 \mu_2)) \tanh(\gamma_1 d_1) \tanh(\gamma_2 d_2)} - 1}{(\sqrt{\mu_1/\epsilon_1} \tanh(\gamma_1 d_1) + (\sqrt{\mu_2/\epsilon_2} \tanh(\gamma_2 d_2))) / \sqrt{((\mu_1 \epsilon_2)/(\epsilon_1 \mu_2)) \tanh(\gamma_1 d_1) \tanh(\gamma_2 d_2)} + 1} \right| \quad (5)$$

Equation (5) is a complex function [21] and numerical evaluation is usually made through mathematical approximations or by software computation. The bilayer design used in this work is composed of a first layer (in contact with PEC) of non-magnetic

material [$\mu_r = (1 - j0)$] with measured, by waveguide method, dielectric constant $\epsilon_r = (10 - j2)$ and 3 mm thickness, and a second layer (between first layer and FS) of non-magnetic material with measured (with software and vector network analyser Agilent 8510C) dielectric constant $\epsilon_r = (6 - j1)$ and 3.5 mm thickness.

With these design parameters, the obtained computer evaluation of RL is showed in Fig. 2, conforming this, the initial expected behaviour of the material to be tested.

3 Experimental results

3.1 Material design

Bearing in mind the intended application sketched in Section 1, the RAM based on the Dallenbach single-layer model [22] or the Salisbury bilayer screen [23] appeared as possible solutions to the above-mentioned conditions (see Fig. 3).

The mechanism presented by Dallenbach comprises a $\lambda/4$ sheet of absorbing material placed on a conducting plane and relies on the destructive interference of the waves reflected from the first and second interfaces. In the case of the Salisbury's model, a second layer which impedance is desirable to be that of the FS ($\approx 377 \Omega$) is deposited over the first. The appearance of materials such as conductive polymers [24, 25] by integrating composite materials [26, 27] and combining them with allotropes of carbon [28, 29] (carbon black or graphite) has allowed to achieve greater absorption bandwidths than those of Dallenbach's materials and an impedance matching as good as that of the Salisbury screen.

In the present case, our RAM was designed to absorb between 11 and 12 GHz using a variation of the Salisbury concept, with a RAM material layer (bottom) having conductivity to improve the absorption and a resistive layer (top) thick enough to form a whole structure that can match the desired absorption frequency. In particular, the bottom layer, of 3 mm thickness, is a compound of commercial silicon rubber loaded to 10% w/w with doped polyaniline [PANI-dodecyl benzene sulphonic acid (DBSA)] of ≈ 1 S/m conductivity, and the top layer, of 3.5 mm thickness, is composed of a commercial silicon rubber loaded to 20% w/w with graphite. In both cases, the grain size is 100 μm . As we see, each layer is a very simple composite, where the only care is to keep the proportions. After that, the RAM will be large-scale reproducible. The resulting compound is a bilayer, flexible, low-cost material scalable without problem up to bigger dimensions.

3.2 Material elaboration

PANI was synthesised through the emulsion method using DBSA in aqueous solution [30]. At first, aniline monomer was distilled. The chemical oxidative polymerisation process of PANI-DBSA uses the ammonium persulphate (APS) as oxidant agent, and the DBSA and hydrochloric acid (HCl) as dopant agents. Then, a specific volume of aniline was added to the recipient containing distilled water, DBSA and HCl with a molar ratio of aniline/(DBSA + HCl) = 1 and magnetic stirring (solution A). On the other hand, a solution containing APS, distilled water and HCl (solution B) was added to solution A, at 0°C. Then, solution A+ solution B was stirred mechanically for 6 h. After that, the sample was allowed to stand for 48 h, washed with distilled water, methanol and acetone several times and dried in vacuum at 60°C for 24 h. The obtained powder was sieved to get 100 μm particles. This powder is mixed uniformly to 10% w/w, with commercial silicon rubber, to then be deposited in a mould where, after 10 h, a flexible sheet is obtained.



Fig. 4 Flexible bilayer RAM sample

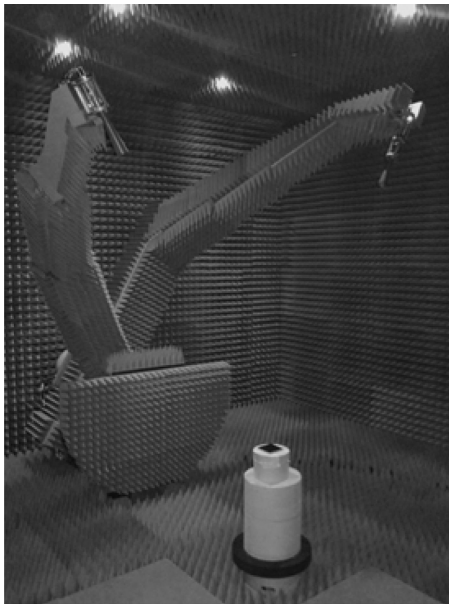


Fig. 5 Set-up of bistatic measurements at BIANCHA

A similar procedure is performed to obtain the graphite sheet to 20% w/w. The 100 μm particle graphite powder is a cheap commercial product that is mainly used as lubricant. Both flexible sheets can be seen in Fig. 4.

3.3 FS measurement

As the RAM will be used under FS conditions, the EM characterisation that comes closest to its actual usage is the one that can be performed in an FS range such as an anechoic chamber of appropriate dimensions. In this paper, the facility called BIANCHA belonging to the National Institute for Aerospace Technology (INTA), Spain was used [31] (see Fig. 5). BIANCHA is a singular facility devised to perform a wide variety of EM tests such as antenna measurements, RCS tests, FS materials characterisation, radar absorption measurements etc. However, apart from this versatility, the most relevant characteristic of BIANCHA is its ability to situate two probes at any point on an imaginary hemisphere and to establish any combination of angles between them and the centre. To achieve this, the system consists of a dual-axis azimuth turntable and two elevated scanning arms, which form a bistatic, spherical field scanner. While one elevated scanning arm is holding the transmitting antenna and travelling on a radius from one horizon to the other, a second elevated scanning arm with the same radius and travel range for the receiving antenna is mounted on the azimuth turntable.

Two main elements are used in the measurements carried out for this paper: on the one hand, a $10 \times 10 \text{ cm}^2$ sample of the material under test (MUT) that can be either the graphite, the PANI or the bilayer compound (graphite + PANI) and, on the other hand, a $10 \times 10 \text{ cm}^2$ flat aluminium plate that will be used, depending on the test, either as a reference or as a metal backing. The MUT and/or the metal plate are always located in the central point of the semi-sphere that encloses all the positions of both antennas with their normal vector pointing to the ceiling of the facility, as shown in Fig. 5. Using these two main elements, three different FS tests were conducted:

- *Absorption*: U.S. Naval Research Laboratory-arch-like [32] comparison measurements [metal reference against metal-backed (MB) MUT] were performed both for normal incidence (monostatic case) and for the bistatic case with 5° , 15° and 25° incidence angles.
- *Permittivity estimation*: An improved version of the MBFS permittivity estimation technique proposed by Ghodangoakar was employed to determine the dielectric characteristics of the different MUT's [33]. The implementation employed at INTA uses particle swarm optimisation (PSO) as the search technique to extract the permittivity from the measured reflection coefficient [34].
- *RCS*: The monostatic RCS at normal incidence was measured for the different MB MUT's.

In all the tests, background subtraction was employed to improve the measurements. Similarly, software gating using the Bohman's window [35] was utilised to keep only the response from the intended target and avoid unwanted reflections. For the transmission and reception of the signals, a 4-port vector network analyser (R&STM ZVA50) was used, emitting and receiving between 7 and 18 GHz. Owing to the software gating, guard bands are recommended at the extremes of the measured bandwidth, so the FS results will be presented from 9 to 16 GHz.

Apart from the FS tests, and in order to compare different measurement methods, waveguide absorption measurements were also performed and are presented in the next section. The absorption measurements in waveguide [36] were made also by comparison of a metal reference (short circuit) against the MB MUT, as shown in the set-up presented in Fig. 6. Bearing in mind the frequencies under study, a type WR-90 or R100 waveguide and adapter were used. Thus, a sample of each material layer and then the final bilayer material in their right order (graphite PANI and short circuit) were carefully placed inside the waveguide (before its end, where the short circuit is placed). Then, the S_{11} parameter was measured for each sample using the same vector network analyser and applying also software gating (Bohman's window) to allow proper result comparisons. Owing to the materials' inherent flexibility, it is worth noting the difficulty in machining the MUT's and placing them into the waveguide.

4 Results and discussion

As mentioned before, three different tests in FS were performed for the MUT's: absorption (monostatic and bistatic), permittivity estimation and monostatic RCS. Those measurements permit to analyse completely the material behaviour in the presence of radiated EM fields and for the intended application, layer by layer as well as for the bilayer sheet developed under the Salisbury's concept [37].

First of all, the normal incidence monostatic absorption measurements are shown in Fig. 7. It can be clearly seen that each separate layer does not show any significant absorption, but working together, as expected by design, absorption resonance appears in the predefined frequencies. This behaviour is typical of these kinds of materials when the electrical permittivity and the material thickness are properly selected.

As the facility easily permits to conduct polarimetric measurements, both θ - θ and θ - ϕ polarisations were measured in order to verify the 'EM inhomogeneity' of the material. In principle, it would be desirable to have a completely

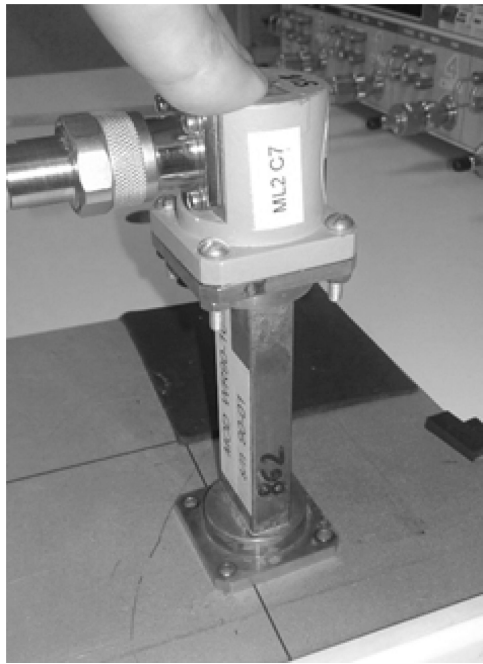


Fig. 6 Set-up for waveguide absorption measurements

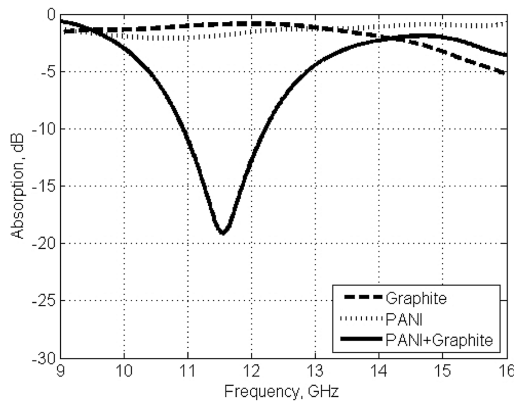


Fig. 7 Single layer versus bilayer absorption

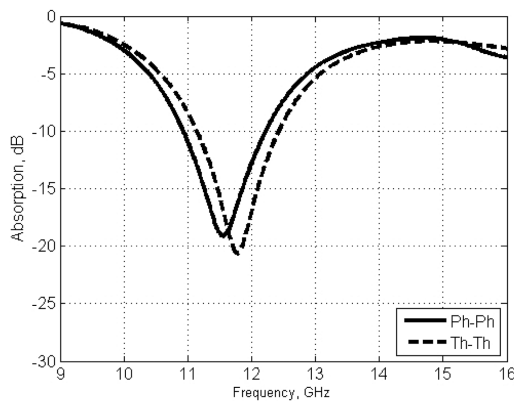


Fig. 8 Absorptions in both polarisations show the EM inhomogeneity

homogeneous material in order to guarantee the expected absorption for any polarisation. Unfortunately, chemical production processes can yield to anomalies producing inhomogeneity.

Then, the characterisation of this irregularity is needed to assure a good performance. In our case, as a consequence of the method of preparation, the EM inhomogeneity is within 3 dB (see Fig. 8), an acceptable value for a 20 dB full absorption RAM.

Second, as depicted in Fig. 9, the specular bistatic absorption measurements carried out show that the behaviour of the material is similar to that of the monostatic case, i.e. it presents a good performance when the angle of incidence goes up to 25°. The little

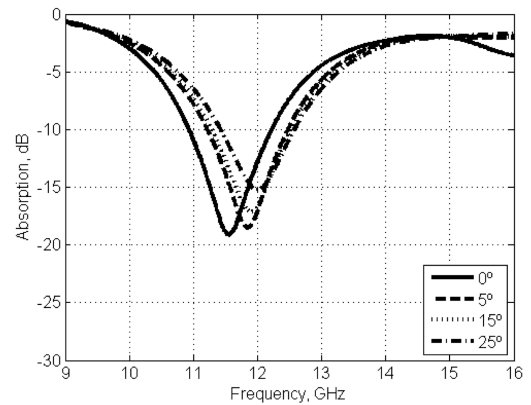


Fig. 9 Comparison between monostatic absorption and bistatic absorption

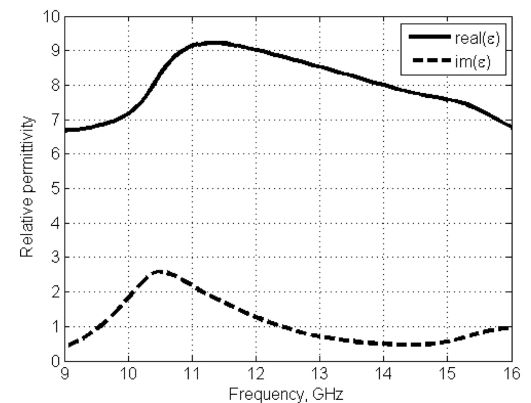


Fig. 10 Electrical permittivity obtained by measuring reflection coefficient and using PSO

frequency variation in the absorption peak is related to the variation in the electric path through the material. Nevertheless, the material retains its design characteristics for the desired spectrum band.

Third, an estimation of the material permittivity was done by measuring the reflection coefficient of the material ended by a metal plate (see Fig. 10). As the material was originally designed as non-magnetic ($\mu_r = 1 - j0$), there is no need to also measure the transmission coefficient and just the reflection one suffices to extract the complex permittivity. The real and imaginary parts of this parameter, depicted in Fig. 10, show the double absorbing phenomena that, combined with the thickness, govern the behaviour of the bilayer compound: frequency resonance and relatively high losses.

As mentioned before, the facility also allows measuring the RCS of the material, backed with a metal plate. Then, using the extracted permittivity, an easy way to validate the results can be done by comparing the normal incidence monostatic RCS measurement results with the values obtained by simulating the same RCS using the ANSYS™ HFSS software. Both values at different frequencies can be compared in Fig. 11, showing an excellent agreement between both curves and validating our measurement approach.

Finally, absorption measurements in the waveguide are presented and compared with the FS ones (see Fig. 12), exhibiting quite remarkable discrepancies. Those differences are due to the fact that for waveguide measurements (in this case WR-90) the thickness of the MUT, the inhomogeneity arisen from the process of developing the compound, and the flexible behaviour of the MUT that prevents its precise machining required to make it fit inside the waveguide, can produce high-order modes, which lead to different results than those obtained for an FS characterisation. These differences confirm that the FS method is better suited for this particular application where the materials will be exposed to radiated fields.

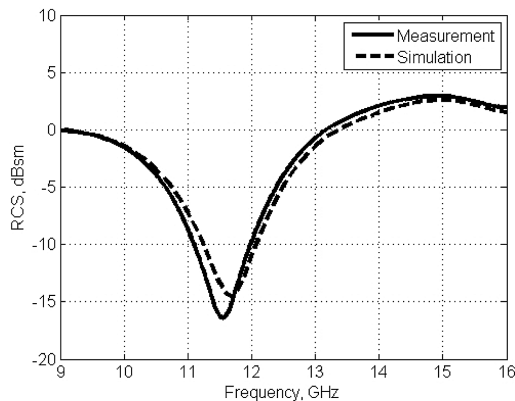


Fig. 11 Comparison between simulated values and FS measured values

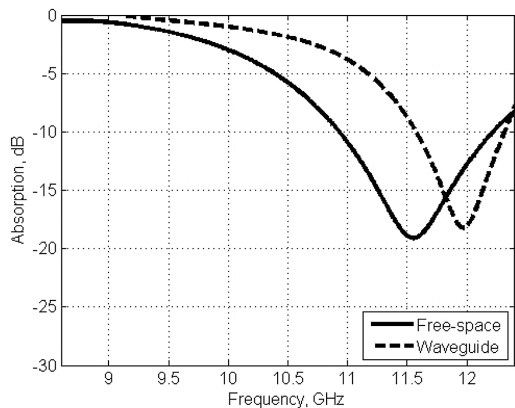


Fig. 12 Absorption differences between waveguide and FS measurements

5 Conclusions

This paper has presented the FS characterisation of a self-developed RAM. The application intended by the authors for this material imposed further restrictions to those already inherent to the aeronautic usage. As a result, the RAM should be flexible and easily scalable from laboratory samples to bigger dimensions at a reasonable cost. As described, such material was developed and this paper focused on electromagnetically characterising it to assess its performance.

The tests were opted to be conducted in the same conditions that the material should encounter in a real operation scenario, it is, in FS. Three different kinds of tests were performed: absorption, permittivity estimation and RCS measurement. They have shown that the material performs well (absorption beyond 20 dB), presents slightly different results depending on the polarisation due to the fabrication process and, finally, it reasonably maintains the behaviour for specular monostatic and bistatic reflections.

The FS measurements have been validated through simulations and it has been proven that this approach is better suited for the characterisation of a material such as the presented in this paper than measuring in waveguides, albeit being such a common practise.

6 Acknowledgments

This study was partially funded by the Spanish Ministry of Economy and Competitiveness (MINECO) within the projects UAVEMI (TEC2013-48414-C3-2-R) and UAVE3 (TEC2016-79214-C3-1-R) and was possible thanks to the Detectability and Electronic Warfare Laboratory of the National Institute for Aerospace Technology (INTA), Spain, the Research and Development Institute for Defense (CITEDEF), Argentina and the National University of San Martín (UNSAM), Argentina.

7 References

- [1] Machinerieen, N.: FR Patent 802728, 1936
- [2] Saville, P.: 'Review of radar absorbing materials'. Technical Memorandum, DRDC Atlantic TM 2005-003, 2005
- [3] Qin, F., Brosseau, C.: 'A review and analysis of microwave absorption in polymer composites filled with carbonaceous particles', *J. Appl. Phys.*, 2012, **111**, p. 061301, doi: <http://dx.doi.org/10.1063/1.3688435>
- [4] Liu, Y., Zhao, X.: 'Study of silicon carbide/graphite double coating polyester woven fabric EMW absorbing property'. IOP Conf. Series: Materials Science and Engineering, 2015, vol. **87**, no. 1, pp. 12076–12082(7), doi: <http://dx.doi.org/10.1088/1757-899X/87/1/012076>
- [5] Choi, W.-H., Shin, J.-H., Song, T.-H., et al.: 'Design of broadband microwave absorber using honeycomb structure', *Electron. Lett.*, 2014, **50**, (4), pp. 292–293, doi: 10.1049/el.2013.3968
- [6] Panwar, R., Agarwala, V., Singh, D.: 'A cost effective solution for development of broadband radar absorbing material using electronic waste', *Ceram. Int.*, 2014, **41**, (2.B), pp. 2923–2930, doi: <http://dx.doi.org/10.1016/j.ceramint.2014.10.118>
- [7] Zabri, S., Cahill, R., Schuchinsky, A.: 'Simpler, low-cost stealth', *Electron. Lett.*, 2015, **51**, (2), p. 127, doi: 10.1049/el.2014.4426
- [8] Micheli, D., Vricella, A., Pastore, R., et al.: 'Multi-layered and multi-functional radar absorbing materials for aeronautical applications: numerical and experimental validation'. Fourth Int. Conf. Multifunctional, Hybrid and Nanomaterials, Sitges, Spain, 2015
- [9] Neo, C., Varadan, V.: 'Optimization of carbon fiber composite for microwave absorber', *IEEE Trans. Electromagn. Compat.*, 2004, **46**, (1), pp. 102–106, doi: 10.1109/TEMC.2004.823618
- [10] De Castro, L., Nohara, E., Faez, R., et al.: 'Dielectric microwave absorbing material processed by impregnation of carbon fiber fabric with polyaniline', *Mater. Res.*, 2007, **10**, (1), pp. 143–150, doi: <http://dx.doi.org/10.1590/S1516-14392007000100020>
- [11] Vinoy, K., Jha, R.: 'Radar absorbing materials: from theory to design and characterization' (Kluwer Academic Publishers, Boston, 1996), p. 150
- [12] Hirano, M., Takahashi, M., Abe, M.: 'A study on reflection coefficient from double layered lossy dielectric by using flanged rectangular waveguide'. IEEE Antennas and Propagation Society Int. Symp., 1999, vol. **1**, pp. 298–301, doi: 10.1109/APS.1999.789139
- [13] Lee, Y., Malek, F., Cheng, E., et al.: 'Experimental determination of the performance of rice husk-carbon nanotube composites for absorbing microwave signals in the frequency range of 12.4–18 GHz', *Prog. Electromagn. Res.*, 2014, **140**, pp. 795–812, doi: 10.2528/PIER13042407
- [14] Baker-Jarvis, J.: 'Transmission/reflection and short-circuit line permittivity measurements'. NIST Technical Note 1341, 1990
- [15] Baker-Jarvis, J., Janezic, M., Riddle, R., et al.: 'Measuring the permittivity and permeability of lossy materials: solids, liquids, metals, building materials, and negative-index materials'. NIST Technical Note 1536, 2004
- [16] Smith, F., Chambers, B., Bennett, J.: 'Methodology for accurate free-space characterization of radar absorbing materials', *IEE Proc. Sci. Meas. Technol.*, 1994, **141**, (6), pp. 538–546, doi: 10.1049/ip-smt:19941154
- [17] Kraus, J., Fleisch, A.: 'Electromagnetics with applications' (McGraw-Hill, Boston, 1999, 5th edn.), pp. 140–141
- [18] Folgueras, M., Alvez, M.E., Faez, R., et al.: 'Dielectric properties of microwave absorbing sheets produced with silicone and polyaniline', *Mater. Res.*, 2010, **13**, (2), pp. 197–201, doi: <http://dx.doi.org/10.1590/S1516-14392010000200013>
- [19] Balanis, C.: 'Advanced engineering electromagnetics' (John Wiley & Sons, USA, 2012, 2nd edn.), pp. 213–215
- [20] MRL Technical Report.: 'Radar absorbing materials – mechanisms and materials', DSTO Materials Research Laboratory, 1989, p. 11
- [21] Huang, Y., Yuan, J., Song, W., et al.: 'Microwave absorbing materials: solutions for real functions under ideal conditions of microwave absorption', *Chin. Phys. Lett.*, 2010, **27**, (2), pp. 197–201, doi: <http://dx.doi.org/10.1088/0256-307X/27/2/027702>
- [22] Dallenbach, W., Kleinsteuber, W.: 'Reflection and absorption of decimeter-waves by plane dielectric layers', *Hochfrequenztechn. Elektroakust.*, 1938, **51**, pp. 152–156
- [23] Salisbury, W.: US Patent 2599944, 1952
- [24] Macdiarmid, A., Chiang, J., Richter, A., et al.: 'Polyaniline: a new concept in conducting polymers', *Synth. Met.*, 1987, **18**, (1–3), pp. 285–290, doi: 10.1016/0379-6779(87)90893-9
- [25] Chandrasekhar, P.: 'Conducting polymers, fundamentals and applications: a practical approach' (Springer US, New York, 1999)
- [26] Wu, K., Ting, T., Wang, G., et al.: 'Effect of carbon black content on electrical and microwave absorbing properties of polyaniline/carbon black nanocomposites', *Polym. Degrad. Stab.*, 2008, **93**, (2), pp. 483–488, doi: 10.1016/j.polymdegradstab.2007.11.009
- [27] De Castro, L., Alves, M., Cerqueira, M.: 'Dielectric properties of microwave absorbing sheets produced with silicone and polyaniline', *Mater. Res.*, 2010, **13**, (2), pp. 197–201, doi: 10.1590/S1516-14392010000200013
- [28] Kwon, S., Ahn, J., Kim, G., et al.: 'Microwave absorbing properties of carbon black/silicone rubber blend', *Polym. Eng. Sci.*, 2002, **42**, (11), pp. 2165–2171, doi: 10.1002/pen.11106
- [29] Oh, J., Oh, K., Kim, C., et al.: 'Design of radar absorbing structures using glass/epoxy composite containing carbon black in X-band frequency ranges', *Compos. B, Eng.*, 2004, **35**, (1), pp. 49–56, doi: 10.1016/j.compositesb.2003.08.011
- [30] Apesteguy, J., Jacobo, S.: 'Synthesis of a soluble polyaniline-ferrite composite: magnetic and electric properties', *J. Mater. Sci.*, 2007, **42**, (17), pp. 7062–7068, doi: 10.1007/s10853-006-1423-7

- [31] Escot, D., Poyatos, D., Aguilar, J., *et al.*: 'Indoor 3D full polarimetric bistatic spherical facility for electromagnetics test', *IEEE Antennas Propag. Mag.*, 2010, **52**, (4), pp. 112–118, doi: 10.1109/MAP.2010.5638248
- [32] Hiatt, R.E., Knott, E.F., Senior, T.B.A.: 'A study of VHF absorbers and anechoic rooms'. Technical Report 5391-1-F, University of Michigan, 1963
- [33] Ghodgaonkar, D., Varadan, V.: 'A free-space method for measurement of dielectric constants and loss tangents at microwave frequencies', *IEEE Trans. Instrum. Meas.*, 1989, **38**, (3), pp. 789–793, doi: 10.1109/19.32194
- [34] Escot, D., Poyatos, D., Montiel, I., *et al.*: 'Soft computing techniques for free-space measurements of complex dielectric constant', *Appl. Comput. Electromagn. Soc. J.*, 2009, **24**, (3), pp. 318–325
- [35] Prabhu, K.: '*Window functions and their applications in signal processing*' (CRC Press, Boca Ratón, 2013)
- [36] Che Seman, F., Cahill, R., Fusco, V.F., *et al.*: 'Design of a Salisbury screen absorber using frequency selective surfaces to improve bandwidth and angular stability performance', *IET Microw. Antennas Propag.*, 2011, **5**, (2), pp. 149–156, doi: 10.1049/iet-map.2010.0072
- [37] Salisbury, W.: US Patent 2599944, 1952